

Extended infrared photoresponse and gain in chalcogen-supersaturated silicon photodiodes

Aurore J. Said,¹ Daniel Recht,¹ Joseph T. Sullivan,² Jeffrey M. Warrender,³ Tonio Buonassisi,² Peter D. Persans,⁴ and Michael J. Aziz^{1,a)}

¹Harvard School of Engineering and Applied Sciences, Cambridge, Massachusetts 02138, USA

²Department of Mechanical Engineering, Massachusetts Institute of Technology, Cambridge, Massachusetts 02139, USA

³ARDEC, Benét Laboratories, Watervliet Arsenal, New York 12189, USA

⁴Department of Physics and Astronomy, Rensselaer Polytechnic Institute, Troy, New York 12180, USA

(Received 12 April 2011; accepted 21 June 2011; published online 17 August 2011)

Highly supersaturated solid solutions of selenium or sulfur in silicon were formed by ion implantation followed by nanosecond pulsed laser melting. n^+p photodiodes fabricated from these materials exhibit gain (external quantum efficiency $>3000\%$) at 12 V of reverse bias and substantial optoelectronic response to light of wavelengths as long as 1250 nm. The amount of gain and the strength of the extended response both decrease with decreasing magnitude of bias voltage, but $>100\%$ external quantum efficiency is observed even at 2 V of reverse bias. The behavior is inconsistent with our expectations for avalanche gain or photoconductive gain. © 2011 American Institute of Physics. [doi:10.1063/1.3609871]

Much effort has been focused on enhancing the magnitude of silicon's photoresponse at near-infrared wavelengths, a spectral range of interest for surveillance, military, and energy device applications. This response is weak because of silicon's indirect band gap of 1.12 eV.¹ Recently, silicon supersaturated with chalcogens prepared by laser irradiation in an SF₆ atmosphere,²⁻⁵ ion-implantation followed by pulsed laser melting,⁶⁻⁸ or pulsed laser mixing⁹ has been shown to be strongly absorbing of sub-bandgap infrared photons. This class of materials is being studied for potential applications in photovoltaics,^{10,11} photodetectors,^{5,12} and light emitters.^{13,14} Here, we report remarkable enhancement of both the range and magnitude of optoelectronic response exhibited by photodiodes with optically flat surfaces prepared by ion implantation with sulfur or selenium ions followed by nanosecond pulsed laser melting.⁶

750 μm thick double-side polished p-type Si(001) wafers with resistivity 10-30 Ω cm were ion implanted at room temperature with either 95keV ³²S⁺ or 176keV ⁷⁸Se⁺, to a dose of 1×10^{16} ions/cm². Ion-implanted samples were then irradiated in air with four pulses from a spatially homogenized, pulsed XeCl⁺ excimer laser (308 nm, 25 ns full width at half maximum, 50 ns pulse duration) with a square spot approximately 3×3 mm². A fluence of 1.7 J/cm² was used for the first three shots to redistribute the dopant more uniformly in depth⁸ and 1.8 J/cm² was used for the fourth shot to ensure that the final melt was the deepest; this prevented exposure of supersaturated material produced in previous shots to non-melting thermal treatment. Laser fluences were calibrated by comparing the measured melt duration of an untreated Si wafer with numerical solutions to the one-dimensional heat equation.^{15,16} Melt duration was monitored *in-situ* via time-resolved reflectivity using a low-power 488 nm Ar⁺ ion laser.¹⁶ Laser melting and the subsequent rapid

solidification form a single-crystal region that retains most of the implanted impurities but that is free of extended defects.^{8,17} This region has the lateral extent of the laser spot and a thickness corresponding to the melt depth (~ 350 nm). The resulting peak sulfur and selenium concentrations are $3 \times 10^{20}/\text{cm}^3$ and $2 \times 10^{20}/\text{cm}^3$, respectively, and the resulting retained doses of sulfur and selenium are $8 \times 10^{15}/\text{cm}^2$ and $7 \times 10^{15}/\text{cm}^2$, respectively.⁸

Figure 1(b) shows a cross-sectional view of a n^+p diode made from a single melted region of an implanted wafer. Treated wafers were first laser cut to a precise square geometry around each 3×3 mm² melted region. At this stage, some samples were furnace annealed in flowing nitrogen for 30 min. Prior to contact deposition, the treated wafers were cleaned in acetone, isopropanol, and deionized water then

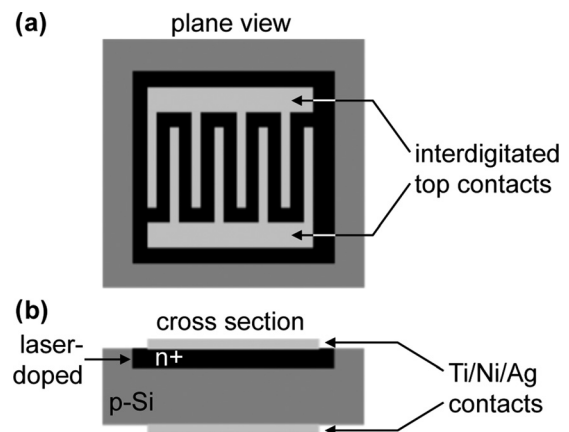


FIG. 1. (a) Top view of an ion-implanted silicon photodiode showing the interdigitated pattern of the top contacts. (b) Cross-sectional schematic diagram of the diode. The substrate wafer (dark gray) is 750 μm thick, and the supersaturated active layer (black) is approximately 350 nm thick over an area of 3×3 mm². The 240 nm thick Ti/Ni/Ag contacts (light gray) are deposited by electron beam evaporation as a comb pattern on the top and as a filled square on the bottom spread on an area of 2.55×2.55 mm².

^{a)}Author to whom correspondence should be addressed. Electronic mail: aziz@seas.harvard.edu.

dipped into a 1:5 HF: H₂O solution. Electron beam evaporation was used to deposit contacts made of titanium (20 nm at a rate of 0.1 nm/s), followed by nickel (20 nm at a rate of 0.1 nm/s), and followed by silver (200 nm at a rate of 0.1 to 0.25 nm/s) on both sides of the sample in a deposition chamber with base pressure between 3 and 8×10^{-7} torr. Shadow masks were employed to create interdigitated contacts (shown in Figure 1(a)) on the top (i.e., the melted side) and a square contact on the back of the sample. Coplanar *I-V* measurements between the top contacts confirmed that they are ohmic. For all measurements reported below, both top contacts were held at the same potential relative to the back contact.

We report steady-state, room-temperature responsivity of these diodes under reverse bias. Light from a 50 W tungsten halide lamp was passed through a monochromator scanned from 400 to 1700 nm in increments of 5 nm. The illuminated area was approximately 3 mm wide \times 1 mm high and was positioned to give maximum photoresponse for each device. The monochromatic light was chopped so that diode response could be measured using a lock-in amplifier. No filters were used from 400 to 750 nm, a 650 nm long-pass filter was used from 700 to 1300 nm, and a high-resistivity anti-reflection-coated silicon wafer was used as an additional filter beyond 1100 nm. The total incident optical power at each wavelength was measured using commercial photodiodes with well-characterized response spectra. A silicon diode was used from 400 to 1000 nm, and a germanium diode was used from 1000 to 1300 nm. All measurements were made using an illumination intensity within an order of magnitude of 0.4 mW/m². The highest intensity occurred at 950 nm. External quantum efficiencies (EQEs) were computed by dividing the measured photocurrent by the incident optical power and then converting to electrons per photon. In all measurements, light was incident on the top surface of samples.

Figure 2 depicts the dependence of external quantum efficiency on reverse bias voltage for a 1×10^{16} sulfur/cm² doped sample that was not furnace annealed. This photodiode shows substantial gain (EQE > 3000%) at 12 V of

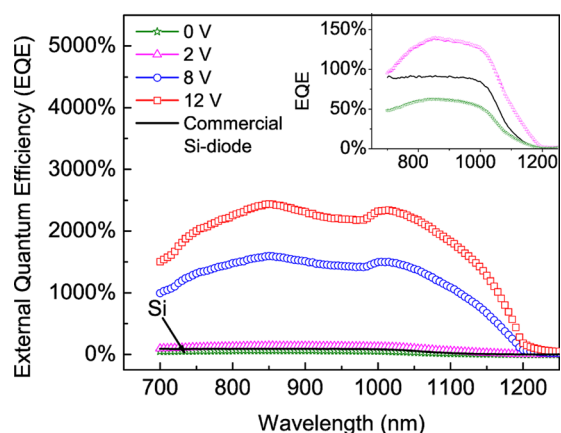


FIG. 2. (Color online) EQE of an un-annealed 1×10^{16} sulfur/cm² doped photodiode for several values of reverse bias voltage. EQE of a commercial Si-photodiode is shown for reference. The inset shows a magnified view of EQE at 0 V and 2 V reverse bias compared to the commercial Si-diode.

reverse bias. This gain decreases with decreasing reverse bias voltage, but EQE > 100% is observed even at 2 V, as can be seen in the inset of Figure 2. The figure also shows the EQE of a commercial silicon photodiode, which did not vary with reverse bias, for comparison.

The cause and physics of gain in this system remain unclear and will be the subject of further research. Nevertheless, the available evidence appears to argue against both avalanche gain and photoconductive gain, at least in their simplest embodiments, as possible mechanisms. Avalanche gain seems to be ruled out by the observation of gain at 2 V of reverse bias. Such a small bias is insufficient to drive appreciable amounts of impact ionization in silicon.¹⁸ The evidence against photoconductive gain is more subtle. The photoconductive gain factor is equal to the carrier lifetime for the carrier type dominating the current divided by the transit time of that carrier type across the device. In a typical silicon pn junction, an increase in the reverse bias voltage will (a) have little effect on the carrier lifetime and (b) cause a linear or sub-linear increase in the carrier transit speed.¹⁹ Accordingly, for a photoconductive mechanism to account for the observed faster-than-linear increase of gain with bias, at least one of the two preceding statements, (a) or (b), must be incorrect. While we have found no evidence to justify rejecting either of these assertions in the case at hand, we recognize that there is some precedent for doing so. Both of these statements have been challenged in discussions of III-V quantum dot photodetectors.^{20,21} In addition, the lifetime could plausibly depend on voltage if the defect energy levels introduced by the sulfur atoms shift (e.g., as with metastable defects^{22,23}) or change occupancy under bias.

Figure 2 also shows that the optoelectronic response of these diodes is extended about 100 nm deeper into the infrared than that of commercial silicon photodiodes. This is more clearly illustrated in Figure 3, which depicts the data from Figure 2 with each curve's maximum normalized to unity. Figure 3 reveals that, like gain, the long-wavelength photoresponse increases with reverse bias voltage. This suggests that gain and extended response might arise from the same physical mechanism.

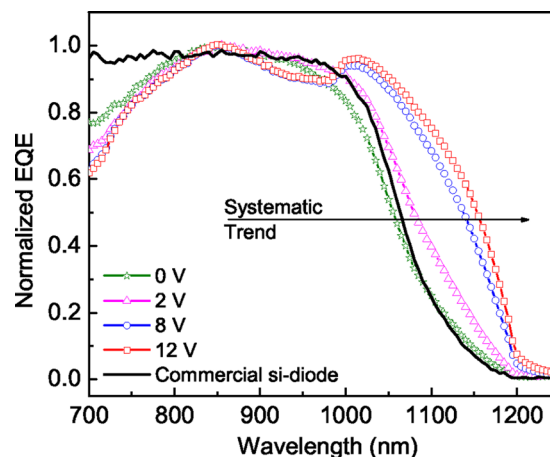


FIG. 3. (Color online) Normalized EQE spectra of an un-annealed 1×10^{16} sulfur/cm² doped photodiode as a function of reverse bias voltage. The extension of photoresponse to wavelengths beyond 1100 nm increases with bias voltage.

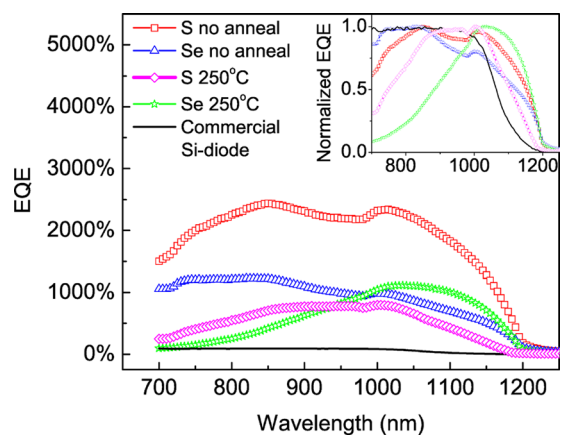


FIG. 4. (Color online) External quantum efficiencies at 12 V reverse bias of un-annealed samples doped with 1×10^{16} sulfur/cm² or 1×10^{16} selenium/cm² and identically prepared samples annealed for 30 min at 250 °C. EQE of a commercial Si-photodiode is shown for reference. Corresponding normalized EQE signals are reported in the inset.

Figure 4 compares the EQE spectra at 12 V reverse bias of un-annealed samples doped with 1×10^{16} sulfur/cm² or 1×10^{16} selenium/cm² with identically prepared samples annealed for 30 min at 250 °C. All diodes exhibit both gain and extended IR response. Normalizing the EQE spectra (as shown in the inset to Figure 4) reveals that the spectra have a range of shapes. An important aspect of this variation is that the EQE from 700 to 850 nm appears to be independent of the EQE at longer wavelengths. Although the samples shown here all received different treatment, it is worth noting that, in a few cases, pairs of samples treated identically showed a similar degree of variation. In addition, preliminary observations suggest that gain and extended IR response are spatially inhomogeneous. Thus, the roles of dopant species, annealing treatment, and inhomogeneity in explaining the observed differences in response spectra remain unclear. These phenomena are the subjects of further investigation.

In summary, we have fabricated n⁺p photodiodes having a thin (~350 nm), supersaturated ($2\text{--}3 \times 10^{20}$ /cm³) n⁺ silicon top layer using ion implantation of sulfur or selenium followed by nanosecond laser melting. These photodiodes display high levels of gain (>3000% at 12 V and >100% at 2 V of reverse bias), along with substantial optoelectronic response at wavelengths as long as 1250 nm. The gain characteristics are not consistent with the behavior we would expect from avalanche gain or photoconductive gain. The mechanism of extended IR response is unclear, but it appears to be correlated with the observation of gain.

The authors acknowledge Nathaniel Berry for technical assistance, Heyun Yin of Varian Semiconductor for ion implantation, and Elif Ertekin, David Hutchinson, Yu-Ting Lin, Bonna Newman, Joseph Paki, Meng-Ju Sher, Jim Carey, and Mark Winkler for helpful discussions. This research was supported in part by the US Army-ARDEC under contract W15QKN-07-P-0092 and by the U.S. Army Research Office under grant W911NF-09-1-0470. A. J. Said acknowledges financial support from the Fulbright Program. D. Recht and J. T. Sullivan were supported by the Department of Defense's National Defense Science and Engineering and the National Science Foundation Graduate Fellowship Programs, respectively. Central facilities were used within the Harvard Center for Nanoscale Systems.

- ¹S. M. Sze, *Physics of Semiconductor Devices*, 2nd ed. (Wiley-Interscience, New York, 1981).
- ²C. Wu, C. H. Crouch, L. Zhao, J. E. Carey, R. Younkin, J. A. Levinson, E. Mazur, R. M. Farrell, P. Gothoskar, and A. Karger, *Appl. Phys. Lett.* **78**, 1850 (2001).
- ³C. H. Crouch, J. E. Carey, J. M. Warrender, E. Mazur, M. J. Aziz, and F. Genin, *Appl. Phys. Lett.* **84**, 1850 (2004).
- ⁴M. A. Sheehy, L. Winston, J. E. Carey, C. M. Friend, and E. Mazur, *Chem. Mater.* **17**, 3582 (2005).
- ⁵J. E. Carey, C. H. Crouch, M. A. Sheehy, M. Shen, C. M. Friend, and E. Mazur, *Opt. Lett.* **30**, 1773 (2005).
- ⁶T. G. Kim, J. M. Warrender, and M. J. Aziz, *Appl. Phys. Lett.* **88**, 241902 (2006).
- ⁷M. Tabbal, T. Kim, J. M. Warrender, M. J. Aziz, B. L. Cardozo, and R. S. Goldman, *J. Vac. Sci. Technol. B* **25**, 1847 (2007).
- ⁸B. P. Bob, A. Kohno, S. Charnvanichborikarn, J. M. Warrender, I. Umez, M. Tabbal, J. S. Williams, and M. J. Aziz, *J. Appl. Phys.* **107**, 123506 (2010).
- ⁹M. Tabbal, T. Kim, D. N. Woolf, B. Shin, and M. J. Aziz, *Appl. Phys. A* **98**, 589 (2010).
- ¹⁰See www.osti.gov/bridge/servlets/purl/984305-ly0Wxh/ for SiOnyx, Inc.'s 6/30/2010 program report to the DOE viewed 2 April 2011.
- ¹¹S. H. Pan, D. Recht, S. Charnvanichborikarn, J. S. Williams, and M. J. Aziz, *Appl. Phys. Lett.* **98**, 121913 (2011).
- ¹²Z. Huang, J. E. Carey, M. Liu, X. Guo, E. Mazur, and J. C. Campbell, *Appl. Phys. Lett.* **89**, 033506 (2006).
- ¹³C. Wu, C. H. Crouch, L. Zhao, and E. Mazur, *Appl. Phys. Lett.* **81**, 1999 (2002).
- ¹⁴M. J. Aziz, C. W. White, J. Narayan, and B. Stritzker, in *Energy Beam-Solid Interactions and Transient Thermal Processing*, edited by V. T. Nguyen and A. G. Cullis (Editions de Physique, Paris, 1985), pp. 231–236.
- ¹⁵J. Bao, M. Tabbal, T. Kim, S. Charnvanichborikarn, J. S. Williams, M. J. Aziz, and F. Capasso, *Opt. Exp.* **15**, 6727 (2007).
- ¹⁶R. Reitano, P. M. Smith, and M. J. Aziz, *J. Appl. Phys.* **76**, 1518 (1994).
- ¹⁷M. J. Aziz, *Metall. Mater. Trans. A* **27**, 671 (1996).
- ¹⁸C. Chang, C. Hu, and R. W. Brodersen, *J. Appl. Phys.*, **57**(2), 302 (1985).
- ¹⁹C. Jacoboni, C. Canali, G. Ottaviani, and A. Alberigi Quaranta, *Solid-State Electron.* **20**(2), 77 (1977).
- ²⁰B. Kochman, A. D. Stiff-Roberts, S. Chakrabarti, J. D. Phillips, S. Krishna, J. Singh, and P. Bhattacharya, *IEEE J. Quant. Electron.* **39**(3), 459 (2003).
- ²¹H. Lim, B. Movaghar, S. Tsao, M. Taguchi, W. Zhang, A. A. Quivy, and M. Razegh, *Phys. Rev. B* **74**, 205321 (2006).
- ²²A. Chantre, *Appl. Phys. A* **48**(1), 3 (1989).
- ²³R. Czaputa, *Appl. Phys. A* **49**(4), 431 (1989).